



Cite this: DOI: 10.1039/d0py01640c

Sustainable thermoplastic elastomers produced via cationic RAFT polymerization†

Scott W. Spring,  Red O. Smith-Sweetser,  Stephanie I. Rosenbloom, 
Renee J. Sifri  and Brett P. Fors *

Plastic production continually increases its share of global oil consumption. Thermoplastic elastomers (TPEs) are a necessary component of many industries, from automotive and construction to healthcare and medical devices. To reduce the environmental burden of TPE production on the world, we developed two new ABA triblock copolymers synthesized through cationic reversible addition–fragmentation chain transfer (RAFT) polymerization from renewable monomers. Using poly(isobutyl vinyl ether) (PIBVE) as the soft block and either poly(*p*-methoxystyrene) (PMOS) or poly(2,3-dihydrofuran) (PDHF) as the hard blocks, we produced triblock copolymers with varying volume fractions and characterized their material properties. PDHF-PIBVE-PDHF is sourced almost entirely from simple alcohols and exhibits mechanical properties comparable to those of commercial TPEs. This effort demonstrates the utility of cationic RAFT for the production of sustainable TPEs.

Received 30th November 2020,

Accepted 13th January 2021

DOI: 10.1039/d0py01640c

rsc.li/polymers

Introduction

Increasing attention in the scientific community has turned to the creation of a renewable plastic economy less reliant on fossil fuels. Currently, over 90% of overall plastic production comes from virgin petroleum feedstock and it is projected that by 2050 plastic production will account for 20% of global oil consumption.¹ Significantly, thermoplastic elastomers (TPEs) represent a 5 million metric ton per year market of such petroleum-based materials.² TPEs possess the elastomeric properties of rubbers and the processability and recyclability of thermoplastics and are commonly used in the automotive, construction, and footwear industries. The decoupling of advanced materials from petroleum feedstock remains a challenge in creating a sustainable plastics economy and requires the development of new renewably sourced polymers that match the physical performance of current TPEs.

TPEs are typified by their ABA copolymer structure composed of a rubbery B-block and glassy A-blocks. At sufficiently low volume fractions of the A-block, microphase separation leads to physical crosslinks formed by discrete glassy domains contained within a continuous phase of the rubbery segment, which affords TPEs their high elongation at break (ϵ_B) and tensile strength at break (σ_B).³ Much of the work to attain TPE properties with renewable ABA copolymers has focused on

ring opening polymerizations of lactones or condensation reactions of carboxylic acids with diols.⁴ Hillmyer and coworkers have developed aliphatic polyester block copolymers, with ϵ_B values in excess of 1000% strain and σ_B values over 30 MPa, comparable with commercial TPEs.^{5–8} Although these polyester-based TPEs exhibit physical properties similar to commercial materials, they are thermally and hydrolytically unstable, leading to desired degradability, but limiting their application. Furthermore, ring opening polymerizations are mostly limited to polyesters and the lactone monomers employed are often several synthetic steps from biomass-derived chemicals. We posited that development of cationic polymerization for production of ABA copolymers would enable renewably sourced vinyl ethers to be incorporated in sustainable TPEs (Fig. 1).

Cationic reversible addition–fragmentation chain-transfer (RAFT) polymerization is an alluring method for producing TPEs, as this method has emerged as an effective technique for polymerizing vinyl ethers in a controlled manner. Cationic RAFT polymerization was first reported by Kamigaito, where the use of chain transfer agents (CTAs) achieves control through a degenerate chain-transfer mechanism.⁹ Recently, our group developed several methods for reversibly oxidizing CTAs using photocatalysts,^{10–13} electrochemical mediators,^{14,15} or chemical oxidants¹⁶ to gain temporal control over cationic polymerizations. Our methods enabled the synthesis of multi-block copolymers; however, they did not possess glassy blocks and, therefore, lacked the aforementioned physical crosslinks that would lead to a TPE. Furthermore, this method only produced block copolymers up to 19 kg mol^{−1}. Consequently, we

Department of Chemistry and Chemical Biology, Cornell University, Ithaca, New York 14853, USA. E-mail: bpf46@cornell.edu

† Electronic supplementary information (ESI) available: Experimental details and general considerations. See DOI: 10.1039/d0py01640c

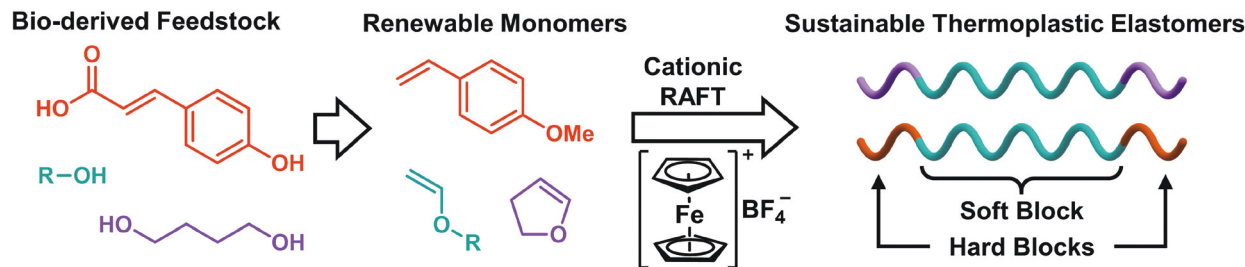


Fig. 1 Synthesis of sustainable TPEs through cationic RAFT polymerization initiated by a chemical oxidant.

set out to identify renewable monomers that could be controllably polymerized *via* a cationic mechanism to produce rubbery and glassy polymers.

Vinyl ethers represent an exciting prospect for renewable polymers because they can be synthesized from widely available bio-derived alcohols. Matsubara and coworkers have demonstrated that calcium carbide is an effective, safe, and renewable alternative to acetylene for the vinylation of alcohols, which we envisaged we could use to make entirely renewable vinyl ether monomers.¹⁷ Importantly, most polyvinyl ethers (PVEs) have low glass transition temperatures (T_g s) making them suitable for use in the rubbery midblock but not the glassy end blocks of TPEs.¹⁸ Hashimoto and coworkers achieved PVE TPEs using poly(2-adamantyl vinyl ether) as the glassy A-blocks; however, because the 2-adamantyl vinyl ether was an expensive and petroleum-derived monomer, we sought other readily available and renewable high T_g polymers accessible by cationic polymerization.^{19,20} We initially identified the cyclic vinyl ether 2,3-dihydrofuran (DHF), because its respective polymer from cationic polymerization possesses a rigid backbone leading to a high T_g of ~ 140 °C.^{21–23} As such, DHF has historically been considered an alluring monomer for glassy polymers.^{24,25} Additionally, DHF can be synthesized with industrially relevant efficiency from biosourced 1,4-butanediol using a heterogeneous catalysis making it an ideal choice for renewable TPEs.^{26,27}

In our initial planning stage of this study we were aware that the controlled polymerization of DHF has previously been a challenge. We anticipated that the cationic polymerization methodology recently developed in our lab could address this challenge; however, we also wanted to pursue other renewable monomers that could undergo cationic polymerization to yield glassy end blocks. To this end, poly(*p*-methoxystyrene) (PMOS) was identified as a candidate which has been used to make PVE-PMOS diblock copolymers.²⁸ Because this monomer is typically derived from petroleum feedstocks, we envisaged an efficient pathway to MOS from renewable coumaric acid, which can be found in many food sources, most notably sugar bagasse, the inedible byproduct of sugar production.^{29,30}

Herein, we disclose our synthesis of renewable ABA block copolymers produced through cationic RAFT polymerization. Our method enables the use of a PVE as the rubbery B-block and either PDHF or PMOS as the glassy A-blocks. All the monomers we employ can be obtained from renewable feedstocks

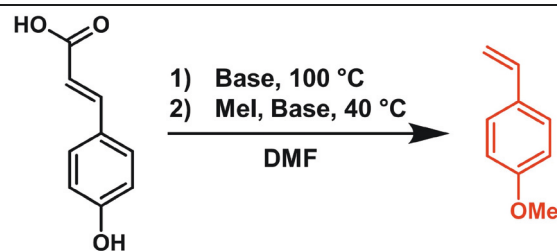
due in part to our development of a two-step synthesis of MOS from coumaric acid. ABA copolymers with high molar masses (70 kg mol^{-1}) are produced utilizing cationic RAFT initiated by a chemical oxidant. In addition, we characterize the mechanical properties and compare them to other renewably sourced TPEs. To this end, we show how cationic polymerization of vinyl ethers enable sustainable TPEs sourced entirely from bio-derived alcohols.

Results and discussion

Synthesis of *p*-methoxystyrene from renewable *p*-coumaric acid

Styrenic block copolymers are the most common TPE and contain glassy polystyrene A-blocks and usually polybutadiene or polyisoprene as the rubbery B-block. To match the material properties of commercial TPEs with sustainable polymers, we posited using a renewable analogue of styrene would provide a starting point for our investigation. We set out to produce MOS, which has been shown to polymerize controllably under cationic conditions and provides a polymer with a high T_g , from coumaric acid.^{31–34} Recently, Kamigaito and coworkers showed that they can decarboxylate ferulic and coumaric acid, which are derived from lignin, using triethylamine and subsequently protect the phenol, enabling controlled radical polymerization.^{35,36} Using a similar strategy, we sought to decarboxylate *p*-coumaric acid and methylate the phenol to produce MOS in a sustainable manner (Table 1). It was also necessary for us to develop a one-pot synthesis from *p*-coumaric acid to avoid the spontaneous polymerization of the *p*-hydroxystyrene.

We first optimized the decarboxylation of coumaric acid to *p*-hydroxystyrene, which has been reported with conventional heating in alkaline aqueous solution and more recently microwave heating with catalytic triethylamine.^{37,38} We found that conventional heating to 80 °C with 2 equivalents of triethylamine achieved high yields when a small amount of butylated hydroxytoluene (BHT) radical inhibitor was added to prevent radical polymerization of the product, *p*-hydroxystyrene (Table 1, entry 1). The use of lower molar equivalents of triethylamine or other bases led to lower yields (Table 1, entries 2–6). Addition of methyl iodide after decarboxylation using the optimized conditions did not give any desired MOS, likely due to triethylamine serving as a favorable nucleophile itself

Table 1 Synthesis of MOS from *p*-coumaric acid, a sugarcane byproduct, in a two-step, one pot procedure


Entry	Base	[Base]/[<i>p</i> -coumaric acid]	Yield (%)
Step 1			
1	NEt ₃	2	95
2	NEt ₃	1	60
3	NEt ₃	0.5	35
4	K ₂ CO ₃	0.5	7
5	K ₃ PO ₄	0.5	11
6	Pyridine	0.5	16
Step 2			
7	NEt ₃	1	0
8	Pyridine	1	0
9	K ₂ CO ₃	1	96
10	K ₃ PO ₄	1	94

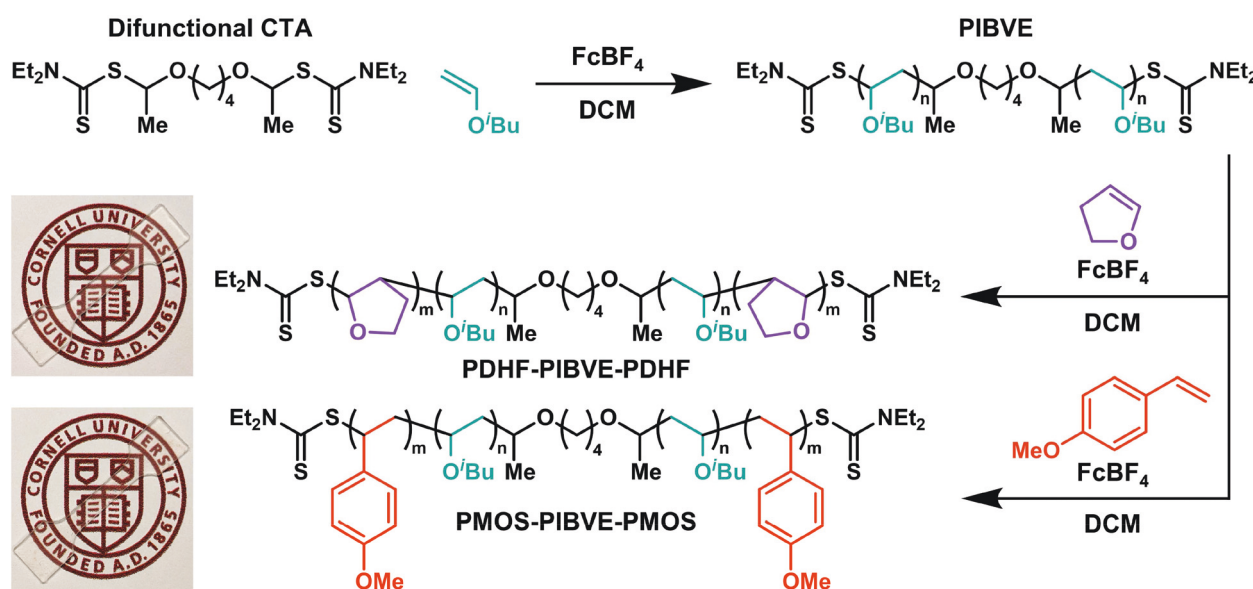
(Table 1, entry 7). To circumvent this, triethylamine was removed *via* rotary evaporation before the addition of a different base and methyl iodide. The transformation was attempted with pyridine as a less nucleophilic base, but led to no conversion (Table 1, entry 8). We found that non-nucleophilic bases such as potassium carbonate and potassium phosphate were required for efficient methylation of *p*-hydroxystyrene (Table 1, entries 9 and 10). The reaction was then performed in a single pot on 25 g scale with triethylamine and

K₂CO₃ in steps 1 and 2, respectively, affording MOS in 77% overall isolated yield.

Synthesis of triblock copolymers

To produce sustainable ABA copolymers from vinyl ethers and MOS, we employed a cationic RAFT polymerization procedure recently developed in our lab.¹⁶ In contrast to the traditional monofunctional CTA used in these polymerizations, we synthesized a difunctional CTA from 1,4-butanediol divinyl ether enabling the production of ABA copolymers in two steps. *iso*-Butyl vinyl ether (IBVE) was polymerized using the difunctional CTA and ferrocenium tetrafluoroborate (FcBF₄) as a catalytic chemical oxidant (Scheme 1) to afford telechelic rubbery PIBVE blocks with various molecular weights and narrow dispersity (*D*) values (see ESI, Fig. S3†). We selected IBVE as our midblock monomer due to its precedent in controlled cationic polymerizations and its renewability. Isobutanol is produced renewably on plant scale under the trade name Butamax®. This bio-derived isobutanol can undergo vinylation with calcium carbide using the method the described vinylation by Matsubara and coworkers to generate IBVE.¹⁷ Notably, the use of FcBF₄ as a chemical oxidant and cationogen allows for the polymerization to proceed at room temperature, improving gelation issues and decreasing the energy demands associated with Lewis or Brønsted acid-initiated polymerizations performed at low temperatures.^{19,20,28,39}

Without isolation of the midblock, telechelic PIBVE was then chain extended with either MOS or DHF to yield PMOS-PIBVE-PMOS or PDHF-PIBVE-PDHF, respectively. The polymerization of a PMOS-PIBVE-PMOS copolymer was monitored over time to elucidate the behavior of the chain extension. We observed a linear increase in *M_n* with respect to monomer conversion over the course of the reaction for both

**Scheme 1** Synthesis of ABA triblock copolymers from a difunctional CTA using cationic RAFT initiated by FcBF₄ as a chemical oxidant. Picture insets show clear and colourless polymers after processing into dogbones.

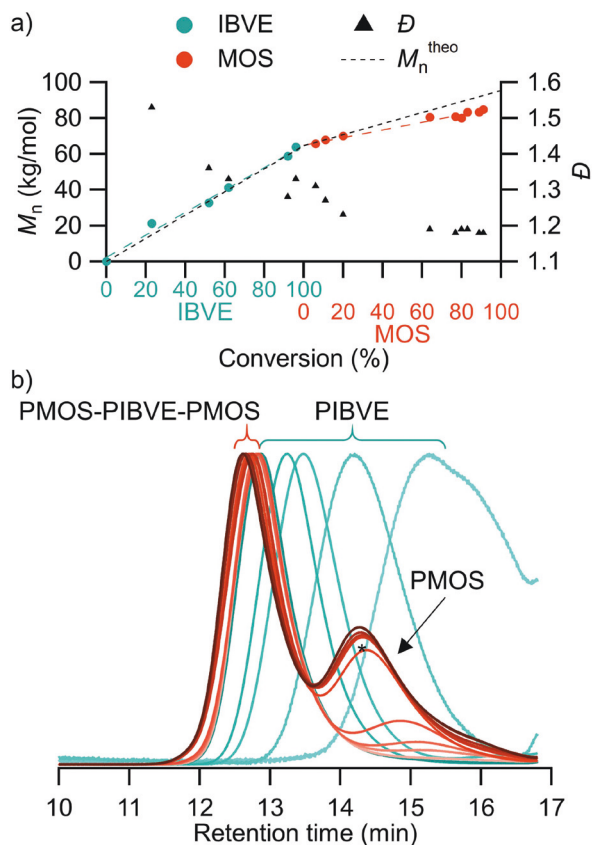


Fig. 2 Polymerization progress in PMOS-PIBVE-PMOS monitored via (a) monomer conversion relative to M_n and \bar{D} and (b) SEC traces showing chain extension and PMOS homopolymer. *Indicates 64% conversion of MOS.

IBVE and MOS (Fig. 2a), which illustrates the “living” character of the polymerization. Fig. 2b shows the gradual shift to higher molecular weight for each block, providing further evidence of the chain extension.

In addition to the chain extension, there emerged a low molecular weight peak we attributed to PMOS homopolymer. We hypothesize that this homopolymer is a result of direct oxidation of the monomer to initiate new chains, a known competitive pathway for cationic RAFT polymerizations.^{12,16} With the IBVE depleted, any new polymer chains must be PMOS.

Due to the increased viscosity upon chain extension, the reaction was diluted and additional FcBF_4 was added to compensate the decreased rate of polymerization (see Experimental section of ESI†). However, the additional FcBF_4 also increases the favorability of adventitious monomer oxidation. We aimed to terminate the polymerizations at 70% conversion of MOS to limit PMOS homopolymer in the final material. This homopolymer could not be fractionally precipitated or otherwise separated from the copolymer.

The volume fraction of hard block (f_{HB}) in each sample was determined by integration of the respective polymer peaks in ^1H NMR (Fig. S10.1–10.6†). Therefore, it should be noted that a portion of the f_{HB} is from homopolymer of PMOS or PDHF in their respective samples. Previous studies of styrenic block copolymers have indicated that added homopolymer of polymer A in an ABA copolymer will evenly distribute within the microphase will not form independent microdomains unless the M_n of homopolymer exceeds that of the midblock.^{40,41} As such, we anticipate that any PMOS or PDHF homopolymer will reside within the discrete glassy domains formed by the end blocks and will not significantly contribute to the mechanical properties of the materials.

We produced a series of each triblock copolymer targeting the same total molecular weight (*ca.* 70 kg mol^{−1}) and varying f_{HB} of hard block (Table 2). The samples are referenced by their hard block polymer and composition as PMOS- f_{HB} or PDHF- f_{HB} . These polymers were easily processed into dogbone-shaped tensile bars using a heated press. Interestingly, unlike most polymers produced from RAFT initiators, our ABA triblock copolymers are clear and colorless (Scheme 1, picture insets). We attribute this to dithiocarbamates being less colored than the dithiobenzoates and trithiocarbonates used in radical RAFT and the high M_n of the polymers reducing dithiocarbamate concentration.⁴²

Material properties

TPEs are typically composed of a two-phase system, where glassy domains are dispersed in a continuous rubbery phase. To determine the morphologies of our samples, small angle X-ray scattering (SAXS) was performed (Fig. S5†) and each sample displayed enough scattering peaks to assign a morphology (Table 2).⁴³ Low f_{HB} samples PMOS-0.21 and PMOS-0.23 display continuous hexagonally packed cylinders

Table 2 ABA copolymer composition and material properties

Entry	Polymer	f_{HB}^a	M_n^b , PIBVE (kg mol ^{−1})	M_n^b , total (kg mol ^{−1})	σ_B (MPa)	ϵ_B (%)	E (MPa)	Morphology ^c
1	PMOS-0.21	0.21	54.1	66	1.4 ± 0.1	405 ± 30	1.2 ± 0.2	HEX
2	PMOS-0.23	0.23	50.0	75	3.1 ± 0.2	340 ± 50	1.2 ± 0.2	HEX
3	PMOS-0.32	0.32	52.5	71	3.3 ± 0.8	126 ± 30	6.3 ± 1	LAM
4	PMOS-0.38	0.38	44.8	68	7.2 ± 0.8	152 ± 9	18 ± 6	LAM
5	PDHF-0.23	0.23	53.0	68	4.3 ± 0.2	570 ± 70	1.3 ± 0.2	HEX
6	PDHF-0.31	0.31	52.0	69	3.4 ± 0.3	335 ± 50	1.9 ± 0.1	HEX

^aTotal volume fraction of the hard block calculated from NMR integration, which includes homopolymer. ^bDetermined by SEC against polystyrene standards. Peaks were defined as seen in Fig. S2† where the reported M_n omits the homopolymer peak. ^cDetermined from the ratios of scattering peaks relative to the principal scattering wavevector, q^* , where HEX = hexagonally packed cylinders and LAM = lamellae.

(HEX) morphology while PMOS-0.32 and PMOS-0.38 adopt a lamellae (LAM) morphology. For the PDHF-PIBVE-PDHF, we only targeted low f_{HB} to achieve HEX morphology, which is well known to give superior TPE properties.^{3,44} Indeed, both samples, PDHF-0.23 and PDHF-0.31, were assigned HEX morphology from their SAXS peaks.

In addition to the assigned morphologies from SAXS, we confirmed phase separation with differential scanning calorimetry (DSC) and dynamic mechanical thermal analysis (DMTA). For sample PMOS-0.38, two T_g s were observed by DSC (-10 °C corresponding to the PIBVE phase and 105 °C corresponding to the PMOS phase), thus confirming the phase separated microstructure (Fig. 3). Similarly, we observed two T_g s for PDHF-0.31; -10 and 126 °C, corresponding to the PIBVE and PDHF phases, respectively. We then attempted to corroborate the high T_g s with temperature sweeps in DMTA. The samples were first subjected to oscillatory strain sweeps from 0.1 to 100% strain at an angular frequency of 1 Hz to establish the linear viscoelastic region (Fig. S6.1 and S6.2†). An oscillatory strain of 0.1% was then applied as the temperature was increased at a rate of 5 °C min^{-1} . A $\tan \delta$ peak at 111 °C was observed in PMOS-0.38, indicative of the PMOS T_g and aligning with our DSC observations (Fig. S6.5†). No $\tan \delta$ peak was observed for PDHF-0.31 from 120 – 170 °C, attributable to the low f_{HB} (Fig. S6.6†).

We next examined the thermal decomposition of our ABA copolymers using thermal gravimetric analysis. Both PMOS-PIBVE-PMOS and PDHF-PIBVE-PDHF containing polymers showed similar decomposition temperatures (T_{d5} , at 5% weight loss) of 346 and 353 °C, respectively (Fig. S7†). These observed T_{d5} s show remarkable thermal stability compared to

other renewable TPEs such as polyesters ($T_d = 260$ °C) and TPEs derived from acrylates or terpenes ($T_d \sim 300$ °C).^{7,45,46} Thermal decomposition of PMOS-PIBVE-PMOS and PDHF-PIBVE-PDHF also occurs well above their upper T_g s (105 and 126 °C), leading to a large melt-processing window.

To characterize the performance of our ABA copolymers as TPEs, we investigated their material properties under tensile strain. The dogbone tensile bars were stretched to break at a strain rate of 0.07 s^{-1} . We first examined the tensile properties of copolymers containing PMOS end blocks (Fig. 4a). Samples PMOS-0.21 and PMOS-0.23 exhibited moderate elongation-at-break (ϵ_B); $405 \pm 30\%$ and $340 \pm 50\%$, respectively. Notably, the stress-at-break (σ_B) for PMOS-0.23 (3.1 MPa) is twice as large as σ_B of PMOS-0.21 (1.4 MPa). For all samples, as f_{HB} increases we observe increased values of tensile strength and Young's modulus (E). The observed elongation is drastically reduced for PMOS-0.32 and PMOS-0.38 ($126 \pm 30\%$ and $152 \pm 9\%$, respectively). Whereas the increase in tensile strength and E is consistent with an increase in f_{HB} , the lower ϵ_B is consistent with the difference in morphological assignments, from PMOS-0.23 with a continuous phase of rubbery PIBVE (HEX), to PMOS-0.32 discontinuous LAM morphology.³

Polymers with PDHF end blocks were synthesized with f_{HB} of 0.23 and 0.31 to examine their elastic behavior. It was

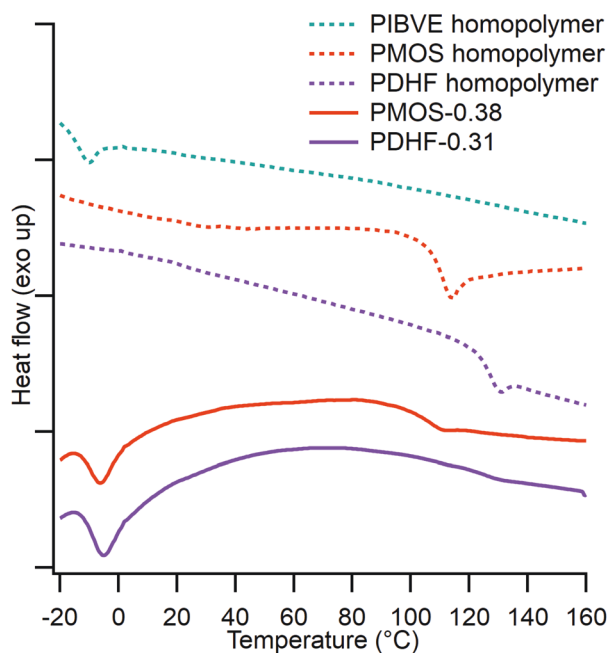


Fig. 3 DSC reveals two T_g s for each ABA copolymer which were consistent with the respective homopolymer T_g s.

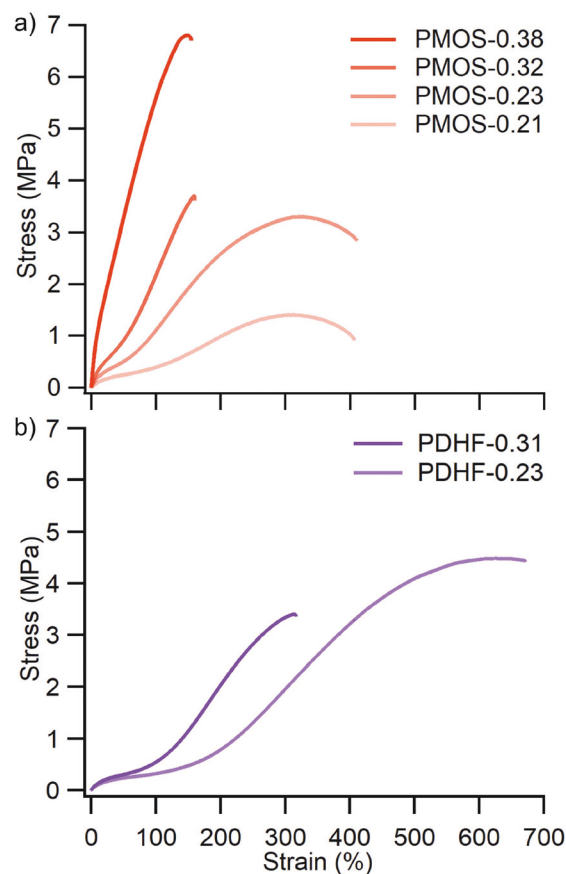


Fig. 4 Representative stress-strain curves of (a) PMOS-PIBVE-PMOS and (b) PDHF-PIBVE-PDHF extended to break.

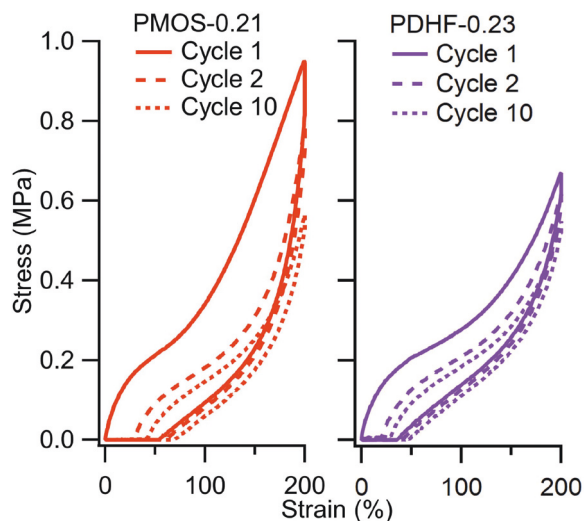


Fig. 5 Cyclic loading and unloading of sustainable TPEs containing (a) PMOS and (b) PDHF end blocks.

observed that both PDHF-0.23 and PDHF-0.31 displayed superior material properties compared to the PMOS samples, achieving higher ϵ_B and σ_B (Fig. 4b). Remarkably, PDHF-0.23 had an observed ϵ_B of $570 \pm 70\%$, higher than any previously reported PVE TPE.^{19,20,39} In addition to increased elongation, PDHF-0.23 shows greater σ_B than PMOS-0.23; 4.3 ± 0.2 MPa compared to 3.1 ± 0.2 MPa, respectively.

A defining characteristic of TPEs is their reversible deformation, which we examined in our elastomeric (high ϵ_B) samples of PMOS-0.21 and PDHF-0.23 using cyclic tensile strains to 200% elongation (Fig. 5). Hysteresis energy is described as the energy difference between the loading and unloading of a polymer and gives insight into the microstructural changes that occur under tension. Both samples show significant energy loss from cycle 1 to 2, but the hysteresis energy stays relatively consistent from cycle 2 to cycle 10. This is likely due to initial breakup and reorientation of the glassy domains during the first cycle and the formation of a preferred microstructure and orientation that remains consistent for the remainder of the cycles.^{47–50} PDHF-0.23 displayed lower hysteresis energy and less energy loss over 10 cycles when compared to PMOS-0.21. Over cycles 2–10, PMOS-0.21 shows a 24% reduction in toughness while PDHF only decreases 13%, where toughness is measured as the total area under the loading curve. Lower energy loss observed for PDHF-0.23 compared to PMOS-0.21 indicates PDHF-PIBVE-PDHF copolymers retain more of their physical properties over repetitive cyclic loads, demonstrating greater recovery after deformation.

Green metrics

Green metrics were evaluated for the synthesis of MOS and the polymerizations of ABA copolymers. Reported in Table S2† are the calculated isolated yields, atom economies (AEs), process mass intensities (PMI), and renewability index (RI). AE evaluates the percent molecular weight of the desired product com-

pared to the molecular weight of all reactants.⁵¹ For an account of all resources required in a process, the PMI was calculated as the mass of product divided by the mass of all reagents, solvents, and catalysts used in the reaction, workup, and purification.^{52,53} We found that while our MOS synthesis provides a renewable route this monomer, it scored low in green metrics due to both steps being quite mass intense. AE was only 44% due to the mass loss from decarboxylation and the loss of iodine in the methylation. The PMI, was high as well, 33 kg kg^{-1} , above other reported PMIs for renewable monomers, such as itaconic acid derivatives.⁵⁴ While this synthesis is not well-optimized in relation to green metrics, it does demonstrate the ability to source MOS, a common monomer in cationic RAFT polymerizations, from biomass.

The polymerizations of PMOS-PIBVE-PMOS and PDHF-PIBVE-PDHF are both ideal in AE, at 100%. This combined with high isolated yields ($>70\%$), highlights the efficiency of our cationic polymerization in producing ABA copolymers. While the PMI for each polymerization is high ($>900 \text{ kg kg}^{-1}$), this comes from the amount of methanol used to crash out the polymer for purification. However, the only byproducts left over are unreacted monomer, solvent, and ferrocene. The unreacted monomer and solvent can be removed under vacuum and, depending on the application of the polymer, the removal of ferrocene (0.07 wt%) would not be required, reducing the PMI by over 200% ($<5 \text{ kg kg}^{-1}$).

Conclusions

We developed a new method for the synthesis of ABA copolymers from sustainable monomers as an avenue toward renewable TPEs. A sustainable, one pot synthetic protocol for MOS from *p*-coumaric acid, a renewable feedstock, was discovered, producing MOS in high yield (77%). Cationic RAFT initiated from a difunctional CTA was employed to first generate well-controlled telechelic PIBVE. Sequential addition of MOS or DHF afforded ABA copolymers of PMOS-PIBVE-PMOS and PDHF-PIBVE-PDHF, respectively. Polymer microphase separation was revealed with DSC and SAXS, the latter enabling assignment of morphology. TGA revealed thermal stability up to 346°C with both PMOS and PDHF compositions. Tensile characterization revealed that while low f_{HB} polymers of both PDHF-PIBVE-PDHF and PMOS-PIBVE-PMOS behave as TPEs, PDHF-IBVE-PDHF possesses superior strength, elongation, and recovery. Specifically, PDHF-0.23 exhibited the highest elongation observed in a PVE TPE ($570 \pm 70\%$). This study demonstrates a significant advance in the cationic RAFT polymerization of vinyl ethers, enabling the production of ABA copolymers with tensile properties well-suited for use as sustainable TPEs.

Conflicts of interest

There are no conflicts to declare.

Acknowledgements

This material is based upon work supported by the National Science Foundation Graduate Research Fellowship Program under Grant No. DGE-1650441. Any opinions, findings, and conclusions or recommendations expressed in this material are those of the author(s) and do not necessarily reflect the views of the National Science Foundation. This work was supported by the National Science Foundation Center for Sustainable Polymers at the University of Minnesota, a Center for Chemical Innovation (CHE-1901635). This work made use of the Cornell Center for Materials Research Shared Facilities that are supported through the NSF MRSEC program (DMR-1120296). This work made use of the NMR Facility at Cornell University that is supported, in part, by the NSF under the award number CHE-1531632. This work is based upon research conducted at the Materials Solutions Network at CHESS (MSN-C) which is supported by the Air Force Research Laboratory under award FA8650-19-2-5220.

Notes and references

- Ellen MacArthur Foundation, *The new plastics economy: Rethinking the future of plastics and catalysing action*, 2017.
- J. G. Drobny, in *Plastics Design Library*, ed. J. G. B. T.-H. of and T. E. Drobny, William Andrew Publishing, Norwich, NY, 2007, pp. 1–8.
- G. Holden, H. R. Kricheldorf and R. P. Quirk, *Thermoplastic Elastomers*, Hanser, 3rd edn, 2004.
- Y. Zhu, C. Romain and C. K. Williams, *Nature*, 2016, **540**, 354–362.
- M. A. Hillmyer and W. B. Tolman, *Acc. Chem. Res.*, 2014, **47**, 2390–2396.
- J. Shin, Y. Lee, W. B. Tolman and M. A. Hillmyer, *Biomacromolecules*, 2012, **13**, 3833–3840.
- A. Watts, N. Kurokawa and M. A. Hillmyer, *Biomacromolecules*, 2017, **18**, 1845–1854.
- A. Watts and M. A. Hillmyer, *Biomacromolecules*, 2019, **20**, 2598–2609.
- M. Uchiyama, K. Satoh and M. Kamigaito, *Angew. Chem., Int. Ed.*, 2015, **54**, 1924–1928.
- V. Kottisch, M. J. Supej and B. P. Fors, *Angew. Chem., Int. Ed.*, 2018, **57**, 8260–8264.
- V. Kottisch, Q. Michaudel and B. P. Fors, *J. Am. Chem. Soc.*, 2017, **139**, 10665–10668.
- V. Kottisch, Q. Michaudel and B. P. Fors, *J. Am. Chem. Soc.*, 2016, **138**, 15535–15538.
- Q. Michaudel, T. Chauviré, V. Kottisch, M. J. Supej, K. J. Stawiasz, L. Shen, W. R. Zipfel, H. D. Abruña, J. H. Freed and B. P. Fors, *J. Am. Chem. Soc.*, 2017, **139**, 15530–15538.
- B. M. Peterson, S. Lin and B. P. Fors, *J. Am. Chem. Soc.*, 2018, **140**, 2076–2079.
- M. J. Supej, B. M. Peterson and B. P. Fors, *Chem*, 2020, **6**, 1794–1803.
- B. M. Peterson, V. Kottisch, M. J. Supej and B. P. Fors, *ACS Cent. Sci.*, 2018, **4**, 1228–1234.
- R. Mataka, Y. Adachi and H. Matsubara, *Green Chem.*, 2016, **18**, 2614–2618.
- T. Hashimoto, T. Namikoshi, S. Irie, M. Urushisaki, T. Sakaguchi, T. Nemoto and S. Isoda, *J. Polym. Sci., Part A: Polym. Chem.*, 2008, **46**, 1902–1906.
- T. Imaeda, T. Hashimoto, S. Irie, M. Urushisaki and T. Sakaguchi, *J. Polym. Sci., Part A: Polym. Chem.*, 2013, **51**, 1796–1807.
- T. Hashimoto, T. Imaeda, S. Irie, M. Urushisaki and T. Sakaguchi, *J. Polym. Sci., Part A: Polym. Chem.*, 2015, **53**, 1114–1124.
- J.-B. Kim and I. Cho, *J. Polym. Sci., Part A: Polym. Chem.*, 1989, **27**, 3733–3744.
- Y. Ogawa, M. Sawamoto and T. Higashimura, *Polym. J.*, 1984, **16**, 415–422.
- F. Sanda and M. Matsumoto, *Macromolecules*, 1995, **28**, 6911–6914.
- O. Nuyken and H. Braun, in *Photoinitiated Polymerization*, American Chemical Society, 2003, vol. 847, pp. 18–213.
- F. Sanda and M. Matsumoto, *J. Appl. Polym. Sci.*, 1996, **59**, 295–299.
- V. Stonkus, K. Edolfa, L. Leite, J. W. Sobczak, L. Plyasova and P. Petrova, *Appl. Catal., A*, 2009, **362**, 147–154.
- L. Leite, V. Stonkus, K. Edolfa, L. Ilieva, L. Plyasova and V. Zaikovskii, *Appl. Catal., A*, 2006, **311**, 86–93.
- T. Higashimura, M. Mitsuhashi and M. Sawamoto, *Macromolecules*, 1979, **12**, 178–182.
- M. Li, Z. Jia, G. Wan, S. Wang and D. Min, *Chem. Pap.*, 2020, **74**, 499–507.
- S. Y. Ou, Y. L. Luo, C. H. Huang and M. Jackson, *Innovative Food Sci. Emerging Technol.*, 2009, **10**, 253–259.
- G. Heublein, S. Spange, M. Sawamoto and T. Higashimura, *Polym. J.*, 1985, **17**, 1085–1090.
- S. Sugihara, S. Okubo and Y. Maeda, *Polym. Chem.*, 2016, **7**, 6854–6863.
- A. J. Perkowski, W. You and D. A. Nicewicz, *J. Am. Chem. Soc.*, 2015, **137**, 7580–7583.
- A. Kanazawa, S. Shibutani, N. Yoshinari, T. Konno, S. Kanaoka and S. Aoshima, *Macromolecules*, 2012, **45**, 7749–7757.
- H. Takeshima, K. Satoh and M. Kamigaito, *Macromolecules*, 2017, **50**, 4206–4216.
- H. Takeshima, K. Satoh and M. Kamigaito, *J. Polym. Sci.*, 2020, **58**, 91–100.
- L. A. Cohen and W. M. Jones, *J. Am. Chem. Soc.*, 1960, **82**, 1907–1911.
- E. Nomura, A. Hosoda, H. Mori and H. Taniguchi, *Green Chem.*, 2005, **7**, 863–866.
- N. Mizuno, K. Satoh, M. Kamigaito and Y. Okamoto, *Macromolecules*, 2006, **39**, 5280–5285.
- X. Quan, I. Gancarz, J. T. Koberstein and G. D. Wignall, *Macromolecules*, 1987, **20**, 1431–1434.
- K. Kimishima, T. Hashimoto and C. D. Han, *Macromolecules*, 1995, **28**, 3842–3853.

- 42 S. Perrier, *Macromolecules*, 2017, **50**, 7433–7447.
- 43 M. W. Matsen and R. B. Thompson, *J. Chem. Phys.*, 1999, **111**, 7139–7146.
- 44 G. Holden, E. T. Bishop and N. R. Legge, *J. Polym. Sci., Part C: Polym. Symp.*, 1969, **26**, 37–57.
- 45 J. Shin, Y. Lee, W. B. Tolman and M. A. Hillmyer, *Biomacromolecules*, 2012, **13**, 3833–3840.
- 46 J. M. Bolton, M. A. Hillmyer and T. R. Hoyer, *ACS Macro Lett.*, 2014, **3**, 717–720.
- 47 T. Pakula, K. Saijo, H. Kawai and T. Hashimoto, *Macromolecules*, 1985, **18**, 1294–1302.
- 48 C. C. Honeker, E. L. Thomas, R. J. Albalak, D. A. Hajduk, S. M. Gruner and M. C. Capel, *Macromolecules*, 2000, **33**, 9395–9406.
- 49 E. M. Frick, A. S. Zalusky and M. A. Hillmyer, *Biomacromolecules*, 2003, **4**, 216–223.
- 50 J. F. Beecher, L. Marker, R. D. Bradford and S. L. Aggarwal, *J. Polym. Sci., Part C: Polym. Symp.*, 1969, **26**, 117–134.
- 51 M. Tobiszewski, M. Marć, A. Gałuszka and J. Namieśnik, *Molecules*, 2015, **20**, 10928–10946.
- 52 C. Jimenez-Gonzalez, C. S. Ponder, Q. B. Broxterman and J. B. Manley, *Org. Process Res. Dev.*, 2011, **15**, 912–917.
- 53 C. Jiménez-González, D. J. C. Constable and C. S. Ponder, *Chem. Soc. Rev.*, 2012, **41**, 1485–1498.
- 54 J. Trotta, A. Watts, A. Wong, A. M. LaPointe, M. A. Hillmyer and B. P. Fors, *ACS Sustainable Chem. Eng.*, 2019, **7**, 2691–2701.